Carbohydrate Polymers 115 (2015) 457–464

Contents lists available at ScienceDirect

Carbohydrate Polymers

journal homepage: www.elsevier.com/locate/carbpol

Preparation and characterization of functionalized cellulose nanocrystals

Assya Boujemaoui, Surinthra Mongkhontreerat, Eva Malmström*, Anna Carlmark*

KTH Royal Institute of Technology, School of Chemical Science and Engineering, Fibre and Polymer Technology, Teknikringen 56, SE-100 44 Stockholm, Sweden

ARTICLE INFO

Article history:
Received 13 June 2014
Received in revised form 22 August 2014
Accepted 25 August 2014
Available online 18 September 2014

Keywords:
Acid hydrolysis
Cellulose nanocrystals
Esterification
Functionalization
Functional organic acid

ABSTRACT

In this work, a series of functional nanocrystals (F-CNCs) was successfully produced by an efficient preparation method, combining acid hydrolysis and Fischer esterification with various organic acids. Functionalities such as ATRP initiators, double bonds, triple bonds, and thiols could be incorporated on CNCs. Surface modification was confirmed by FT-IR, XPS, and elemental analysis. Physical properties of F-CNCs were assessed by AFM, XRD and TGA. Moreover, ATRP initiator functionalized CNCs were utilized to graft poly(methyl methacrylate) via ATRP, thiol functionalized CNCs were reacted with Ellman's reagent to determine the thiol content and dye disperse red 13 was attached to alkyne functionalized CNCs to estimate the propiolate content. The herein presented method is a highly versatile and straightforward procedure for the preparation of F-CNCs which is believed to be a better alternative for the commonly utilized, extensive, multistep, and time consuming post functionalization methods.

1. Introduction

During the last decade, cellulose nanocrystals (CNCs) have attracted great interest, in both industry and academia, owing to their low density, renewability, biodegradability, high reinforcing capability, lower production cost compared to glass and carbon nanofibers, and their vast applicability (Mariano, El Kissi, & Dufresne, 2014). CNCs were originally prepared by acid hydrolysis employing strong acids, mainly sulfuric and hydrochloric acids (Rånby, 1951). The acid hydrolysis conditions has thereafter been optimized in order to improve the recovery yield and to tailor the CNCs dimensions (Bondeson, Mathew, & Oksman, 2006). Recently, phosphoric acid was utilized to prepare CNCs (Camarero Espinosa, Kuhnt, Foster, & Weder, 2013). Several other preparation methods have been reported, such as combination of acid and enzymatic hydrolysis (Siqueira, Tapin-Lingua, Bras, da Silva Perez, & Dufresne, 2010), TEMPO oxidation (Hirota, Tamura, Saito, & Isogai, 2010; Qin, Tong, Chin, & Zhou, 2011), ammonium persulfate oxidation (Leung et al., 2011), ionic liquid hydrolysis (Man et al., 2011), and gaseous acid hydrolysis (Nuopponen, Meriluoto, & Kontturi, 2012).

However, acid hydrolysis is the most widely used procedure for the production of CNCs. CNCs exhibit a high specific surface area that implicates more available hydroxyl groups on their surface and subsequently offers great possibility for chemical modification (Dufresne, 2012).

The application potential of CNCs can be significantly enhanced by surface modification (Eichhorn, 2011). A series of surface modified CNCs with outstanding properties has previously been prepared either by covalent or non-covalent chemical modification approaches (Habibi, 2014). The non-covalent approach is based on the adsorption of surfactants to the cellulose surface and can be accomplished via ionic or non-ionic interactions. This method is used mainly to improve the dispersibility of CNCs in organic solvents and hydrophobic matrices (Aloulou, Boufi, & Beneventi, 2004; Ben Azouz, Ramires, Van den Fonteyne, El Kissi, & Dufresne, 2011; Cranston & Gray, 2006; Habibi, Hoeger, Kelley, & Rojas, 2009; Kim et al., 2009; Salajková, Berglund, & Zhou, 2012).

For the covalent modification, small molecules or polymers are reacted with the hydroxyl groups on the glucose units. For example, CNC surfaces have been modified by grafting of polyesters (poly(ε-caprolactone and polylactide) via ring-opening polymerization of cyclic esters utilizing the OH-group as an initiating function (Carlmark, Larsson, & Malmström, 2012). Moreover, different functional groups have been attached to CNC surfaces, such as initiators for reversible deactivation radical polymerization (RDRP), (Morandi, Heath, & Thielemans, 2009; Yi, Xu, Zhang, & Zhang, 2009; Zoppe et al., 2010) allyl, thiol, alkyne, and azide functionalities for click chemistry reactions (Filpponen & Argyropoulos, 2010; Huang, Li, & Gray, 2014; Sadeghifar, Filpponen, Clarke, Brougham,

* Corresponding authors. Tel.: +46 8 7908027 (AC), +46 8 7907225 (EM).
E-mail addresses: mavem@kth.se (E. Malmström), annac@kth.se (A. Carlmark).

http://dx.doi.org/10.1016/j.carbpol.2014.08.110
0144-8617/

& Argyropoulos, 2011; Tingaut, Hauert, & Zimmermann, 2011) via esterification reaction of available hydroxyl groups of cellulose with acid halides. Amine groups were also grafted on CNCs surface via esterification reaction followed by thiol-ene Michael addition (Nielsen, Eyley, Thielemans, & Aylott, 2010). Furthermore, functionalized CNCs can be employed for polymer grafting via RDRP, to enhance the compatibility of CNCs and a hosting matrix, fluorescent labeling of CNCs for bioimaging applications, cellulosic photo responsive nano-arrays (Filpponen, Sadeghifar, & Argyropoulos, 2011), as well as several other applications (Biyani, Foster, & Weder, 2013; Kelly et al., 2013; Khan et al., 2013; Shopsowitz, Hamad, & MacLachlan, 2011). However, the above mentioned functionalities have all been prepared by the reaction of already produced CNCs. To introduce functionalities on already prepared CNCs, multiple steps and tedious liquid exchange from water to an appropriate reaction solvent, purification and then re-dispersion are commonly required. In this procedure, typically, unmodified CNCs are prepared by acid hydrolysis of cellulose fibers in an initial step, followed by solvent exchange into organic solvents or freeze drying and re-dispersion, and then, in a second step, the CNCs are post-functionalized to attach the functional group. In a previous study by Dorgan et al., simultaneous Fisher esterification and acid hydrolysis were performed in order to produce functional cellulose nanocrystals (F-CNCs) but this approach was only applied for introducing acetate and butyrate groups (Braun & Dorgan, 2008).

The aim of this study was to prepare a series of F-CNCs where the functionality is introduced onto the CNCs already in the production step, by utilizing functional organic acids. In this simple and versatile manner, modified CNCs bearing functional groups such as; double and triple bonds, thiols and a bromo-ester group (i.e. initiator for atom transfer radical polymerization, ATRP) were produced in relatively high yields (46–62 wt%) (Braun & Dorgan, 2008). We hypothesize that the surface functionalization of CNCs involves Fischer esterification and hydrolysis reactions. Consequently F-CNCs could be directly obtained in a one-step reaction, thus omitting extra functionalization steps and tedious solvent exchange. The properties and reactivity of F-CNCs were also investigated. We believe this study to be of utmost importance for the chemical modification of CNCs and hence for the production of functional CNCs. The incorporated functionalities allow for CNCs to be utilized in composite applications, either compatibilizing the surface of the fibers with the matrix material, or by introducing cross-linkable groups. Furthermore, the CNCs functionalized with an ATRP-initiator could be polymerized with a plethora of functional polymers, resulting in new and interesting materials.

2. Experimental and methods

2.1. Materials

Filter paper (Whatman no. 1) was employed as a cellulose source and used without further purification. 2-Bromopropionic acid (BPA), 3-mercaptopropionic acid (MPA), 4-pentenoic acid (PA), 2-propynoic acid (PyA), 37% hydrochloric acid (HCl), ethanol (EtOH), dichloromethane (DCM), tetrahydrofuran (THF), methanol (MeOH), ethyl 2-bromopropionate (EBP), *N*,*N*,*N*′,*N*″,*N*″-pentamethyldiethylenetriamine (PMDETA), copper(I)bromide, copper sulfate, and sodium ascorbate, were purchased from Sigma Aldrich and used as received. Methyl methacrylate (MMA) was passed through a column of neutral aluminum oxide prior to polymerization reaction to ensure the inhibitor removal. Azide functionalized dispersed red 13 (DR13-N_3) was synthesis as described elsewhere (Malkoch et al., 2005).

2.2. Instrumentation

Size exclusion chromatography (SEC) with dimethyl formamide (DMF) as mobile phase was utilized to determine molecular weights and molar-mass dispersities. The analyses were performed on a TOSOH EcoSEC HLC-8320 GPC system equipped with an EcoSEC RI detector and three columns (PSS PFG 5 μm; Microguard, 100 Å, and 300 Å) (MW resolving range: 100–300,000 g mol^{-1}) from PSS GmbH, using DMF (0.2 mL min^{-1}) with 0.01 M LiBr as the mobile phase at 50 °C. A conventional calibration method was created using narrow, linear poly(methyl methacrylate) standards ranging from 700 to 2000,000 g mol^{-1}. Corrections for flow rate fluctuations were made using toluene as an internal standard. PSS WinGPC Unity software version 7.2 was used to process data.

IR spectroscopy was performed on a Perkin-Elmer Spectrum 2000 FT-IR equipped with a MKII Golden Gate, Single Reflection ATR system from Specac Ltd, London, U.K. All spectra were normalized against a specific ATR crystal absorption region (2300–1900 cm^{-1}).

Proton Nuclear Magnetic Resonance (^{1}H NMR) was conducted on a Bruker AM 400 at 400 MHz using deuturated chloroform ($CDCl_3$) as solvent to determine the conversion of the non-grafted PMMA. The solvent signal was used as an internal standard. The molecular weight ($M_{n,th}$) of PMMA chains was estimated from the degree of polymerization (DP) assessed by ^{1}H NMR.

Atomic force microscopy (AFM) with tapping-mode AFM (Multimode IIIa, Veeco Instruments, Santa Barbara, CA) was utilized to determine the CNCs dimensions. Diluted CNCs water dispersions were applied on modified surface mica with poly L-lysine 1% and the excess was washed with Milli-Q water. The sample surfaces were dried with air flow and scanned with a cantilever having a tip radius <10 μm and typical spring constant 40 N m^{-1}.

XPS spectra were collected with Axis Ultra DLD electron spectrometer (Kratos Analytical Ltd, UK) using monochromatized Al *K*α (1486.6 eV) source operated at 150 W. Survey spectra were collected from 1100 to 0 eV at pass energy of 160 eV. High resolution C1s, O1s, N1s, S2p and Br3d spectra were collected at pass energy of 20 eV with a scan step of 0.1 eV. In order to minimize possible X-ray induced degradation of the samples, C1s and O1s spectra were measured within first 10 min of exposure. Kratos software was used for spectra processing. High-resolution XPS spectra were fitted using linear combinations of 70:30 Gauss–Lorentzian functions on Shirley background-subtracted spectra. Binding energy (BE) scale was calibrated using aliphatic C1s component, set at 285.0 eV.

XRD diffractograms were collected utilizing a Siemens D5000 diffractometer with a Cu *K*α monochromatic radiation generated at 40 kV and 30 mA (λ = 0.15405 nm). The samples were scanned at 2θ angular range 10–60° and the increment was 0.02°. The plotted diffractograms are represented from 2θ angular range 10–40° as there was no useful information in the range of 40–60°. The crystallinity index was calculated according to the following equation:

$$\mathrm{CrI} = \left(1 - \frac{I_{\mathrm{Am}}}{I_{002}} \times 100\right) \quad (1)$$

where I_{002} is the maximum intensity of the (0 0 2) lattice peak and I_{Am} is the corresponding intensity of the amorphous part at 18°.

Cellulose crystals width can be estimated according to Scherrer equation,

$$W = \frac{K\lambda}{\Delta\theta \times \cos\theta} \quad (2)$$

where W represents the width of the crystals, K a dimensionless shape factor usually taken as 0.9, λ is the wavelength used for the measurement, $\Delta\theta$ is the width at (0 0 2) half peak, and θ is the angle for the (0 0 2) lattice reflection.

Elemental analysis was performed at Institut des Sciences Analytiques, Lyon. The degree of substitution (DS) was calculated according to Eq. (3). For samples 2-BPA–CNC and 3-MPA–CNC, the calculation of DS was based on the content of bromine and sulfur, respectively, and for samples containing only carbon, oxygen and hydrogen the calculations were based on the content of carbon.

$$DS = \frac{162x - M_Y N_{Y(AGU)}}{M_Y \times N_{Y(R)} - M_R \times x} \quad (3)$$

where x is the weight fraction of an element Y in the analyzed sample, M_Y and M_R are the molecular weights of the element Y and the grafted group, respectively, and $N_{Y(AGU)}$ and $N_{Y(R)}$ are the number of atoms of element Y in the repeating D-anhydroglucopyranose unit (AGU) and in the grafted group (R).

2.3. Method and procedure

2.3.1. Preparation of unmodified cellulose nanocrystals (HCl-CNC)

Unmodified cellulose nanocrystals (HCl-CNC) were prepared similarly to Van den Berg, Schroeter, Capadona, and Weder (2007). Grounded filter paper (10 g) was dispersed in HCl (300 ml, 3 M) and immersed in an oil bath preheated to 110 °C for 90 min under magnetic stirring. The HCl-CNC was recovered by diluting the reaction mixture 10 times with deionized water followed by filtration. The HCl-CNC was thoroughly washed through repeated filtration and re-dispersion until neutral pH, then ultrasonicated and finally freeze dried.

2.3.2. Preparation of functionalized cellulose nanocrystals (F-CNCs)

In a typical procedure, 0.50 g of grounded cellulose fibers (filter paper Whatman no. 1) was added to a 50 ml round-bottomed flask equipped with a magnetic stirrer, thereafter deionized water (11.25 ml) was added. The flask was immersed in ice/water bath and HCl (3.75 ml, conc (37%)) was added drop wise to obtain a final solution of 3 M. After the addition of HCl, the round-bottomed flask containing the reaction mixture was immersed in a preaheated oil bath at 110 °C for 15 min. Thereafter, the mixture was filtered over a glass filter (pore size 1) and the retentate was washed with deionized water until a neutral pH was reached. Thereafter, the cellulose fibers were further hydrolyzed with 10 ml of a functional acid (2-propynoic acid, 4-pentenoic acid, 2-bromopropionic acid, or 3-mercaptopropionic acid) under reflux for 4 h. The hydrolysis was stopped by diluting the system ten times with deionized water, then filtered over glass filter (pore 4), and thoroughly washed with deionized water until a neutral pH was reached. The obtained suspension was collected, diluted with deionized water to obtain a total volume of 250 ml, sonicated for 30 min using 28% as amplitude and then freeze dried. Functionalized CNCs were denoted: 2-PyA-CNC (for 2-propynoic acid hydrolysis), 4-PA-CNC (for 4-pentenoic acid hydrolysis), 2-BPA-CNC (for 2-bromopropanoic acid hydrolysis), and 3-MPA-CNC (for 3-mercaptopropionic acid hydrolysis).

2.3.3. Grafting of poly(methyl methacrylate) (PMMA) on 2-BPA-CNC

2-BPA-CNC (0.200 g) was dispersed in 2.5 g anisole in a 10 ml round-bottomed flask equipped with a magnetic stirrer and the dispersion was sonicated in a sonication bath for 5 min prior to the reaction. After stirring overnight MMA (5.0 g, 50 mmol) was added, and the reaction was kept in an ice/water bath to avoid premature polymerization while adding the other reagents EBP (56.0 mg, 0.335 mmol) and PMDETA (58 mg, 0.335 mmol) were added to the mixture. Thereafter, the flask was degassed by one vacuum/argon cycle where after Cu(I)Br (4.80 mg, 0.033 mmol) was added under argon flow. Finally, the round-bottomed flask was sealed with rubber septum, degassed with 2 vacuum/argon cycles and then immersed in an oil bath preheated to 90 °C. After a set reaction time (0.25 h, 1 h, and 4 h for 15%, 31%, and 45% monomer conversion, respectively) the reaction was stopped by exposing the reaction mixture to air and diluting the reaction mixture with DCM. The polymer-grafted CNCs (PMMA-g-CNCs) were separated and purified from the free polymer by dispersing the reaction mixture in DCM and then filtering. The grafted PMMA-g-CNCs were purified individually by Soxhlet extraction with THF for 24 h to remove any unbounded free polymer, then with methanol for 24 h to remove remains of copper. The free polymer was passed through neutral aluminum oxide to remove copper then precipitated in cold methanol, filtrated over glass filter (pore 4) and finally dried under vacuum at 50 °C overnight.

2.3.4. Azide–alkyne Huisgen cycloaddition of DR13-N_3 on 2-PyA-CNC

2-PyA-CNC (100 mg) was dispersed in MeOH (43.75 ml) in an E-flask overnight and then ultrasonicated for 5 min using amplitude of 28%. Copper sulfate (5.90 mg, 0.037 mmol), sodium ascorbate (14.70 mg, 0.074 mmol), and azide functionalized dispersed red 13 (DR13-N_3) (18.10 mg, 0.037 mmol in 6.75 ml DCM) were added to the reaction mixture. The E-flask was kept in dark under stirring for 24 h. The 2-PyA-CNC was thereafter washed thoroughly using a mixture of MeOH/DCM (43.75 ml/6.75 ml) then Soxhlet extracted with DCM for 24 h to remove any unreacted DR13-N_3.

3. Results and discussion

3.1. Characterization of functionalized cellulose nanocrystals

The concurrent Fischer esterification and acid hydrolysis have previously been applied for surface modification and preparation of acetate- and butyrate-modified cellulose nanocrystals (Braun & Dorgan, 2008). However, this methodology has never been performed for the production of functional cellulose nanocrystals (F-CNCs).

In this study, several F-CNCs, carrying different functional groups, have successfully been synthesized by simultaneous acid hydrolysis and esterification using different functional organic acids. In the initial attempts, neat organic acids were utilized for the acid hydrolysis of cotton fibers (filter paper), which resulted in CNCs having the required functionality incorporated into the structure. However, when solely the functional acid was utilized, reaction times were long, up to 10 days for some of the acids. For this reason, either hydrochloric acid (HCl) or hydrobromic acid (HBr) was added to the hydrolysis step to reduce the reaction time. This did indeed reduce the time for hydrolysis, but caused undesired cleavage of the functional group. Due to this, we elaborated a pretreatment step with hydrochloric acid prior to the addition of the functional acid. This was found to reduce the time for hydrolysis considerably and the resulting F-CNCs retained the desired functionality. The short pre-treatment step represents the optimal conditions for the successful production of several F-CNCs utilizing different functional acids.

3.1.1. Morphology

Fig. 1 illustrates a scheme describing the production pathway of functional cellulose nanocrylstals. Functionalities such as; double and triple bonds, thiols and a bromo-ester group capable of initiating ATRP, were successfully introduced to the CNCs during the production step. Noteworthy, the most commonly used ATRP initiator (i.e. ethyl α-bromoisobutyrate, tertiary *initiator*) could not be attached on cellulose nanocrystals surface utilizing the herein described reaction protocol with α-bromoisobutyric acid.

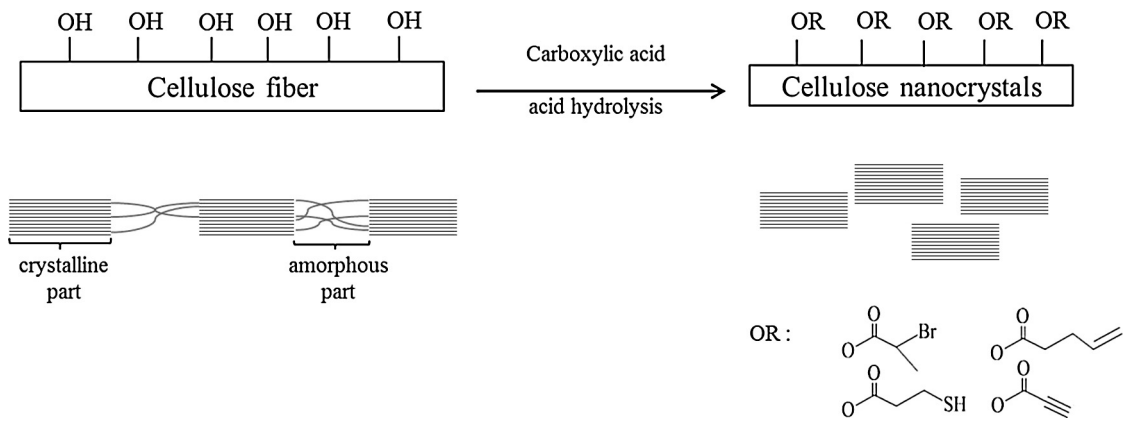

Fig. 1. Acid hydrolysis and esterification of cellulose fibers employing either 2-bromopropionic acid, 3-mercaptopropionic acid, 4-pentenoic acid or 2-propynoic acid.

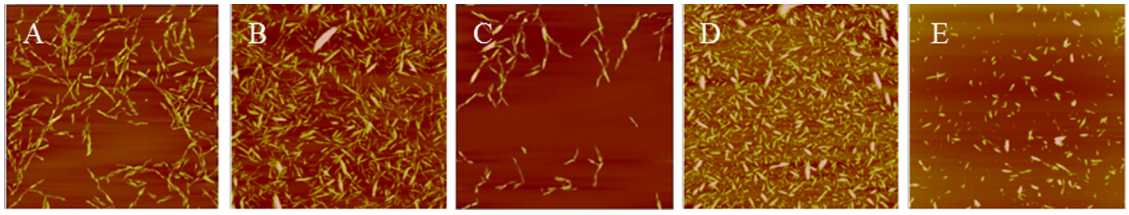

Fig. 2. AFM images of F-CNCs produced from: (A) hydrochloric acid (HCl-CNC), (B) 2-propynoic acid (PyA-CNC), (C) 2-bromopropionic acid (2-BPA-CNC) (D) 3-mercaptopropionic acid (3-MPA-CNC), (E) 4-pentenoic acid (4-PA-CNC). The micrograph size is 5 × 5 μm.

Table 1
Functional carboxylic acids employed for the production of functionalized cellulose nanocrystals (F-CNCs), yields and dimensions of F-CNCs obtained from AFM image analysis.

Carboxylic acid	F-CNCs	Yield (%)	Particle dimensions	
			Length (nm)	Width (nm)
2-Propynoic acid	2-PyA-CNC	62	200 ± 80	13.6 ± 3.5
2-Bromopropanoic acid	2-BPA-CNC	46	249 ± 75	18.2 ± 4.3
3-Mercaptopropionic acid	3-MPA-CNC	50	197 ± 45	18.2 ± 12.6
4-Pentenoic acid	4-PA-CNC	48	175 ± 42	13.2 ± 3.4

CNCs were indeed obtained utilizing this acid, but the bromo-functionality was lost, most probably due to hydrolysis during the reaction. However, when 2-bromopropionic acid was employed instead, the bromo-functionality was retained, resulting in the attachment of a secondary ATRP-initiator. The sizes of the F-CNCs were roughly estimated using AFM imaging (Fig. 2) and were found to be approximately 14–18 nm in width and 175–250 nm in length (Table 1), which correlates to previously reported results for CNCs from cotton fibers (Dufresne, 2012). The broad size distribution of F-CNCs could be attributed to the fact that no further isolation (apart from filtration) of CNCs, was used, i.e. no centrifugation.

X-ray diffraction measurements were performed for the starting material (filter paper), CNCs obtained by hydrochloric acid hydrolysis (HCl-CNC), and all of the F-CNCs, in order to study and elucidate the effect of the chemical modification on the crystallinity. Table 2 summarizes the crystallinity index and the width of the crystals, and Fig. 3 illustrates the XRD diffractograms. The F-CNCs and HCl-CNC diffractograms show distinct peaks around 34.5°, 22.8°, 16.5°, and 14.7°, characteristic of Cellulose I which suggests that the cellulose nanofibers did not undergo any substantial structural changes during the production. As expected, the crystallinity index increased after acid hydrolysis for most of the acids used, except for 4-pentenoic acid where the crystallinity decreased dramatically (4-PA-CNC), indicating substantial morphological change of the CNCs during the hydrolysis. In an earlier study by Sassi and Chanzy (1995) it was demonstrated that when the number of acetylated groups becomes substantial, this caused the modified fibrils to partly detach from the crystalline structure, which in turn decreases the crystallinity of the final modified crystals. Similarly, the surface of 4-PA-CNCs is assumed to be highly substituted using 4-pentenoic acid. This assumption could be further confirmed from the results of elemental analysis where the highest degree of substitution was obtained for 4-PA-CNC (Table 4). Moreover, the increased hydrophobic character of the grafted group compared to the other functionalities could increase the peeling effect of substituted chains from the crystal surface.

The width of the F-CNCs could also be estimated from XRD measurements, following Scherrer equation, Table 2. The obtained

Table 2
Crystallinity index (CrI) and crystal width dimension (W) of filter paper, HCl-CNC, and functionalized cellulose nanocrystals obtained from XRD measurements. The abbreviations used in the table; 2-bromopropanoic acid (2-BPA), 4-pentenoic acid (4-PA), 3-mercaptopropionic acid (3-MPA), and 2-propynoic acid (2-PyA).

	CrI (%)	*W* (nm)
Filter paper	71	8.6
HCl-CNC	77	7.4
2-BPA-CNC	78	10.1
4-PA-CNC	65	10.1
3-MPA-CNC	81	9.1
2-PyA-CNC	74	8.0

Table 3
Atomic percentages and carbon deconvolution of unmodified CNCs and functionalized CNCs determined by High Resolution XPS of C1s. The abbreviations used in the table; 2-bromopropanoic acid (2-BPA), 4-pentenoic acid (4-PA), 3-mercaptopropionic acid (3-MPA), and 2-propynoic acid (2-PyA).

Sample	C %	O %	Br %	S %	C—C %	C—O %	O—C—O %	O—C=O %
HCl-CNC	61.6	37.8	–	–	5.2	44.5	11.1	0.8
2-BPA-CNC	62.3	37.3	0.3	–	5.2	44.3	11.1	1.7
4-PA-CNC	62.7	36.4	–	–	8.7	41.8	11.0	1.2
3-MPA-CNC	60.5	38.4	–	1.0	2.4	45.0	11.3	1.8
2-PyA-CNC	62.3	37.7	–	–	5.1	44.4	10.9	1.2

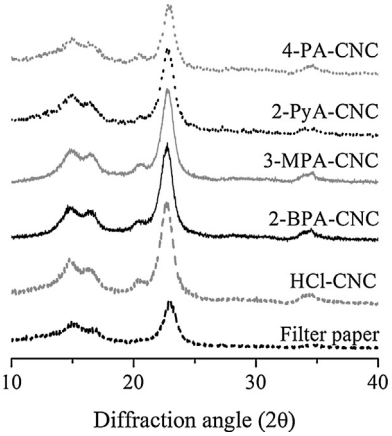

Fig. 3. XRD diffractograms of filter paper, cellulose nanocrystals obtained by hydrochloric acid (HCl-CNC) and various organic acids. The abbreviations used in the spectra; 2-bromopropanoic acid (2-BPA), 3-mercaptopropionic acid (3-MPA), 2-propynoic acid (2-PyA), and 4-pentenoic acid (4-PA).

values are in the same range as the reported values from AFM, Table 1.

3.1.2. Surface characterization

The successful surface modification of CNCs was confirmed using IR spectroscopy where a peak around 1730 cm^{-1}, ascribed to the carbonyl group which forms during the esterification reaction, can clearly be observed (Fig. 4). Unfortunately, other characteristic peaks for the complementary different functionalities (e.g. thiol, alkene and alkyne) could not be clearly distinguished utilizing this method due to interference with cellulose peaks in the region 1675–600 cm^{-1}. A possible side reaction during Fischer esterification condition utilizing 3-mercaptopropionic acid could be homopolymerization. However it is worth mentioning that no traces of homopolymerization could be observed. This observation was further corroborated by XPS analysis results where no increase of C—C bond percentage, that could indicate the formation of polymer chains, was noticed for any of the samples, except for 4-PA-CNC where an increase was expected due to the chemical structure of the grafted group having four C—C bonds.

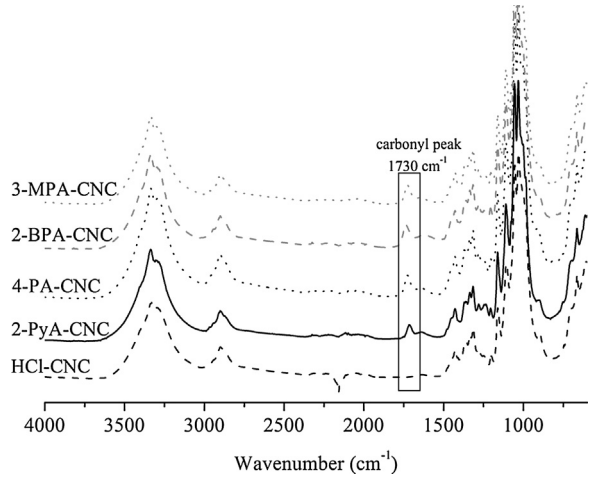

Fig. 4. FTIR spectra of F-CNCs compared to neat cellulose nanocrystals (HCl-CNC). The abbreviations used in the spectra; 2-propynoic acid (2-PyA), 4-pentenoic acid (4-PA), 2-bromopropanoic acid (2-BPA) and 3-mercaptopropionic acid (3-MPA).

The F-CNCs were analyzed by XPS and compared to CNCs produced utilizing standard procedure, i.e. by acid hydrolysis utilizing HCl, herein denoted HCl-CNC. The results are summarized in Table 3, showing that the contribution of carbonyl functionality to the C1s peak is slightly higher compared to the one from HCl-CNC. Binding energies of various bonds, wide XPS spectra and deconvoluted C1s spectra of HCl-CNC and F-CNCs are presented in Table S1, Figs. S1 and S2, respectively. The contribution of the carbonyl functionality to the C1s peak for HCl-CNC is believed to be attributed to impurities (hydrolysis degradation products) and oxidation of end groups of cellulose chains (Dufresne, 2012). Furthermore, the appearance of bromine and sulfur in 2-BPA-CNC and 3-MPA-CNC, respectively, confirms the successful attachment of functionalities bearing bromine or sulfur on the CNCs surface. By converting the atomic percentage of bromine and sulfur in samples 2-BPA-CNC and 3-MPA-CNC to weight percentage, the bromine and sulfur content are found to be 1.75% and 2.42% respectively. The low percentage of bromine in 2-BPA-CNC obtained from XPS results compared to the results from elemental analysis, where the bromide content was 2.85%, is believed to be due to the sensitivity of bromide to XPS analysis as shown by Rieke, Baer, Fryxell, Engelhard, and Porter (1993). Another important observation is the increase of the C—C percentage in case of 4-PA-CNC (8.7%) which is due to the grafting of a molecule containing a higher number of aliphatic carbons (4 C—C bonds) as compared to the other functionalities.

Elemental analysis was performed in order to further confirm the success of surface functionalization utilizing various organic acids and to determine the degree of substitution. The results are summarized in Table 4. The obtained results were corrected based on the theoretical percentages of carbon, oxygen and hydrogen in cellulose. The degrees of substitution were estimated based on Eq. (3) and were found to vary between 0.06 and 0.27, depending on the organic acid utilized for the acid hydrolysis. One hypothesis to the variation in DS could be attributed to the acidity of the acids utilized. However, no correlation between the degree of substitutions and p*K*a values was observed in this study. Another assumption

Table 4
Elemental composition by weight, degree of substitution (DS) of cellulose nanocrystals prepared by hydrochloric acid hydrolysis (HCl-CNC), and functionalized cellulose nanocrystals (F-CNCs). The abbreviations used in the table; 2-bromopropanoic acid (2-BPA), 4-pentenoic acid (4-PA), 3-mercaptopropionic acid (3-MPA), and 2-propynoic acid (2-PyA).

	C %	O %	H %	Br %	S %	DS
HCl-CNC	44.44	49.38	6.17			
2-BPA-CNC	43.87	47.25	6.02	2.86	–	0.06
4-PA-CNC	47.86	45.67	6.47	–	-	0.27
3-MPA-CNC	44.74	46.96	6.12	–	2.17	0.12
2-PyA-CNC	45.84	47.97	6.19	–	–	0.19

to explain the dissimilarity in DS could be swelling of cellulose and viscosity of various acids and also steric hindrance when 2-bromopropionic acid was employed.

3.1.3. Thermal stability

Surface functionalization of CNCs could influence the thermal stability (Dufresne, 2012), as is demonstrated for CNCs with carboxylate and sulfate esters attached to their surface. CNCs prepared by sulfuric acid hydrolysis undergo decomposition starting at 150 °C, which is explained by the presence of sulfate ester groups, which form sulfuric acid upon heating and subsequently catalyze the hydrolysis and degradation of cellulose chains (Camarero Espinosa et al., 2013). Fig. S3 represents thermograms from TG analysis and first derivative thermograms of F-CNCs. The degradation temperature depends on the functional group attached to the CNCs surface. The first derivative of TG traces shows one sharp decomposition peak for almost all F-CNCs closer to the one of HCl-CNC at 320 °C. F-CNCs prepared with 3-mercaptopropionic acid and 2-bromopropionic acid exhibited the lowest degradation temperatures, most likely due to the presence of thiol and bromine moieties on their surfaces, which could generate corrosive species upon heating and consequently accelerate the degradation process of cellulose. It is noteworthy that the degradation temperatures of 2-BPA-CNC and 3-MPA-CNC (303 °C and 294 °C, respectively) are much higher compared to CNCs prepared by sulfuric acid hydrolysis which is believed to be of great interest when high processing temperatures are necessary.

3.2. Efficiency of functionalized cellulose nanocrystals

In order to investigate the potential of the functional groups attached, the F-CNCs were used for further functionalizations. 2-BPA-CNC was employed for ATRP of methyl methacrylate (MMA) to yield PMMA-g-CNCs; 3-MPA-CNC was reacted with Ellman's reagent to assess the amount of double bonds on the surface, and 2-PyA-CNC was reacted with an azide-functional dye, utilizing the copper catalyzed Huisgen cycloaddition reaction.

2-BPA-CNC, a CNC prepared utilizing 2-bromopropanoic acid, was employed for surface-initiated ATRP (SI-ATRP) grafting of MMA, using standard ATRP-conditions. The grafting of PMMA chains was confirmed with IR spectroscopy (Fig. S4), where a clear increase in the carbonyl peak was observed, attributed to the carbonyl groups in PMMA. Different reaction times were investigated and, as expected, the carbonyl peak was found to increase with increasing reaction time. A free, sacrificial, initiator, in this case EBP which is a secondary initiator, equivalent to the one attached to the surface of the CNCs, was added to the polymerization solution and the molecular weight of the grafted PMMA on CNCs surface was assumed to be similar to the molecular weight of the free forming polymer (Hansson, Antoni, Bergenudd, & Malmström, 2011). Theoretical molecular weights calculated based on NMR, Mn and molar-mass dispersity ($Đ_M$) obtained from DMF-SEC for different PMMA lengths are summarized in Table S2. The molecular weights of the free polymer obtained from DMF-SEC are higher compared to the theoretical values even though the SEC is calibrated against PMMA standards. This could be due to poorer control over the polymerization using a secondary ATRP initiator, employed in this case, which is further highlighted by the slightly higher molar-mass dispersity. By optimizing the ATRP conditions, the control of the polymerization, and effectively the grafting, could be increased, but this lies outside the scope of this paper, as the grafting was performed solely to show the efficiency of the F-CNCs.

XPS analysis was performed on PMMA grafted cellulose nanocrystals in order to further confirm the grafting of PMMA on CNCs surface. XPS elemental spectra of PMMA-g-CNCs (Fig. S5) show two distinguished signals assigned to carbon in the region 285–289 eV, and to oxygen in the region between 532 and 533 eV. Details regarding contribution from O—C=O, O—C—O, O—C, C—C, and C—COO bonds from C1s deconvoluted signal obtained from high resolution XPS of C1s are represented in Figure S6 and percentages of each bond contribution are summarized in Table S3. All the samples showed slightly similar bond contribution from the C1s signal, suggesting that mainly PMMA is present in the surface layer of all samples.

The grafting of PMMA from CNCs surface increased the thermal stability of CNCs, as can be seen from the thermograms in Fig. S7. The thermal degradation temperature of PMMA-g-CNCs-increased by increasing the amount of grafted PMMA. Similar observations have also been reported elsewhere for PMMA-g-cellulose nanocrystals as well as for other polymers (Dufresne, 2012). Moreover, the amount of grafted PMMA on CNC could be estimated from TGA results. The PMMA-grafted CNC contained 38 wt%, 39 wt%, and 44 wt% of PMMA in $PMMA_{15}$-g-CNC, $PMMA_{31}$-g-CNC, and $PMMA_{45}$-g-CNC, respectively. The high PMMA loading of CNCs after polymerization is believed to be due to its high specific surface area.

Ellman's reagent was utilized to quantify the concentration of thiol groups on 3-MPA-CNC. Ellman's reagent (5,5′-dithiobis-(2-nitrobenzoic acid) reacts selectively with thiols to generate 2-nitro-5-thiobenzoate which is a chromophore that absorbs at 412 nm (Scheme S1).

The obtained result showed that the thiol content was 766 $\mu mol\ g^{-1}$. This number can be compared to a previous study by our group (Hansson et al., 2013), where the thiol content was investigated on the surface of filter paper or microcrystalline cellulose (after the attachment and subsequent cleavage of a similar, initiating group) and found to be around 18–40 $\mu mol\ g^{-1}$. As expected, the value obtained from the thiol-functionalized CNCs prepared herein was significantly higher, due to the inherent higher surface area of CNCs. Calculating the DS based on the thiol content, a value of 0.12 was obtained which is similar to the one calculated from elemental analysis (Table 4). This observation indicates that only hydroxyl groups located on the CNC surface have been modified. DS calculation details based on Ellman's reaction can be found in the supporting information.

In previous studies, dyes have been attached to the surface of CNCs by a range of different chemistries; for example, fluorescein-5′-isothiocyanate (FTIC) or Rhodamine B isothiocyanate (RBITC) were attached to CNC's surface via the reaction of isothiocyanate with available hydroxyl group on CNC's surface (Nielsen et al., 2010). The average amount of isothiocyanate dyes attached to CNCs was estimated by UV–vis and fluorescence spectroscopy to be in the range of 2.8 $\mu mol\ g^{-1}$ and 2.1 $\mu mol\ g^{-1}$ for FTIC and RBITC, respectively. Moreover, the succinimidyl ester dye has been attached to CNCs surface via a three-step process where, in an initial step, a double bond was introduced via esterification, followed by thiol-ene Michael addition to attach amine functionality which was subsequently coupled with the succinimidyl ester functionality of the dye. The average amount of succinimidyl ester dye attached to CNCs surface was determined by UV–vis spectroscopy. Up to 10.4 $\mu mol\ g^{-1}$ dye was attached to CNCs.

Herein, azide functionalized disperse red 13 (DR13-N_3) was successfully attached to 2-PyA-CNC through a copper-catalyzed Huisgen cycloaddition, in order to determine the alkyne content. This 'click reaction' between an alkyne and an azide is reported as robust, selective and efficient, leading to high yields (Hein, Liu, & Wang, 2008). The F-CNCs turned red after the reaction and retained this color even after purification by Soxhlet extraction with DCM for 24 h, confirming the successful covalent attachment of DR13-N_3. A blank reaction was conducted, employing the same reaction conditions for the 'click-reaction', on HCl-CNC. In this case, no dye should

be incorporated as the HCl-CNC did not contain any alkyne groups. A dispersion of HCl-CNC with the same CNCs weight percentage as for the dye grafted CNCs (DR13-g-CNC) dispersion (0.05 wt%) was used as blank for the UV–vis analysis and the absorbance was measured at 495 nm (Fig. S8). The blank sample showed no absorbance at 495 nm while DR13-g-CNC absorbed. Assuming that the yield of azide–alkyne Huisgen is 100%, the amount of propiolate group grafted to CNC-2-PyA was estimated to be 335 $\mu mol\,g^{-1}$. The DS could be back calculated from the content of propiolate group similarly to the DS from Ellman's reaction, and the value obtained was 0.05 which is much lower than DS calculated from elemental analysis (0.19). This observation could be attributed both to steric hindrance due to the chemical structure of DR13, and also to the reliability of the UV–vis analysis conducted on CNCs suspension and not on a clear solution.

In order to investigate the ene-functionalized CNCs, attempts were performed to react a thiol-functional disperse red, utilizing the highly versatile thiol-ene reaction. The resulting CNCs exhibited color after the reaction, which indicate a successful coupling. However, when performing a blank reaction with the same dye, utilizing HCl-CNC, it was noticed that unspecific binding occurred. This is most probably due to reaction of the thiol-groups with the carboxylic acid groups present in HCl-CNC, or could be caused by physiosorption. For this reason, unfortunately, the ene-functionality could not be quantified in the same manner as the thiol- and triple bond functionalities within the framework of this study. However, as indicated with both IR spectroscopy and XPS, the ene-functionality has most probably been incorporated onto the surface of the CNCs, similarly to the other functionalities.

4. Conclusions

Several functional CNCs have been produced by the simultaneous hydrolysis and Fisher esterification using functional organic acids. Four different acids were investigated, 2-propynoic acid, 4-pentenoic acid, 2-bromopropionic acid, and 3-mercaptopropionic acid. All of the obtained F-CNCs showed a clear carbonyl peak around 1730 cm^{-1} in IR spectroscopy originating from the formed ester bond between the CNC and the functional group. The F-CNCs were 14–18 nm in width and 175–250 nm in length according to AFM. Thermal analysis revealed that F-CNCs had similar, or even higher thermal stability, compared to CNCs obtained with hydrochloric acid and sulfuric acid, respectively. The ATRP initiator functionalized CNCs (2-BPA-CNC) were successfully grafted with PMMA via SI-ATRP. The grafted CNCs exhibit a higher thermal stability compared to 2-BPA-CNC. The thiol functionalized CNCs (3-MPA-CNC) were reacted with Ellman's reagent and the thiol content was determined to be as high as 766 $\mu mol\,g^{-1}$. Moreover, the alkyne functionalized CNCs (PyA-CNC) were reacted with azide-functional dispersed red 13 through azide–alkyne Huisgen cycloaddition and the amount of functional group was roughly estimated to be around 335 $\mu mol\,g^{-1}$. The proposed procedure could most probably be applied to any cellulose source, and it is believed to be an efficient and straightforward method for direct production of functional CNCs with high functionality content compared to the commonly tedious pathway of CNCs post functionalization, hence expanding the utilization and possible commercialization of such materials.

Acknowledgements

The authors would like to thank Wilhelm Beckers Jubileumsfond for financial support and Dr Micheala Salajková is acknowledged for assistance with AFM sample preparation. Dr Samuel Pendergraph is thanked for assistance with the TOC image. The manuscript was written through contributions of all authors. All authors have given approval to the final version of the manuscript.

Appendix A. Supplementary data

Supplementary material related to this article can be found, in the online version, at http://dx.doi.org/10.1016/j.carbpol.2014.08.110.

References

Aloulou, F., Boufi, S., & Beneventi, D. (2004). Adsorption of organic compounds onto polyelectrolyte immobilized-surfactant aggregates on cellulosic fibers. *Journal of Colloid and Interface Science*, *280*(2), 350–358.

Ben Azouz, K., Ramires, E. C., Van den Fonteyne, W., El Kissi, N., & Dufresne, A. (2011). Simple method for the melt extrusion of a cellulose nanocrystal reinforced hydrophobic polymer. *ACS Macro Letters*, *1*(1), 236–240.

Biyani, M. V., Foster, E. J., & Weder, C. (2013). Light-healable supramolecular nanocomposites based on modified cellulose nanocrystals. *ACS Macro Letters*, *2*(3), 236–240.

Bondeson, D., Mathew, A., & Oksman, K. (2006). Optimization of the isolation of nanocrystals from microcrystalline cellulose by acid hydrolysis. *Cellulose*, *13*(2), 171–180.

Braun, B., & Dorgan, J. R. (2008). Single-step method for the isolation and surface functionalization of cellulosic nanowhiskers. *Biomacromolecules*, *10*(2), 334–341.

Camarero Espinosa, S., Kuhnt, T., Foster, E. J., & Weder, C. (2013). Isolation of thermally stable cellulose nanocrystals by phosphoric acid hydrolysis. *Biomacromolecules*, *14*(4), 1223–1230.

Carlmark, A., Larsson, E., & Malmström, E. (2012). Grafting of cellulose by ring-opening polymerization—A review. *European Polymer Journal*, *48*(10), 1646–1659.

Cranston, E. D., & Gray, D. G. (2006). Morphological and optical characterization of polyelectrolyte multilayers incorporating nanocrystalline cellulose. *Biomacromolecules*, *7*(9), 2522–2530.

Dufresne, A. (2012). *Nanocellulose: From nature to high performance tailored materials*. Berlin: Walter de Gruyter GmbH.

Eichhorn, S. J. (2011). Cellulose nanowhiskers: promising materials for advanced applications. *Soft Matter*, *7*(2), 303–315.

Filpponen, I., & Argyropoulos, D. S. (2010). Regular linking of cellulose nanocrystals via click chemistry: Synthesis and formation of cellulose nanoplatelet gels. *Biomacromolecules*, *11*(4), 1060–1066.

Filpponen, I., Sadeghifar, H., & Argyropoulos, D. S. (2011). Photoresponsive cellulose nanocrystals. *Nanomaterials and Nanotechnology*, *1*(1), 34–43.

Habibi, Y. (2014). Key advances in the chemical modification of nanocelluloses. *Chemical Society Reviews*, *43*(5), 1519–1542.

Habibi, Y., Hoeger, I., Kelley, S. S., & Rojas, O. J. (2009). Development of Langmuir–Schaeffer cellulose nanocrystal monolayers and their interfacial behaviors. *Langmuir*, *26*(2), 990–1001.

Hansson, S., Antoni, P., Bergenudd, H., & Malmström, E. (2011). Selective cleavage of polymer grafts from solid surfaces: Assessment of initiator content and polymer characteristics. *Polymer Chemistry*, *2*(3), 556–558.

Hansson, S., Trouillet, V., Tischer, T., Goldmann, A. S., Carlmark, A., Barner-Kowollik, C., et al. (2013). Grafting efficiency of synthetic polymers onto biomaterials: A comparative study of grafting- from versus grafting-to. *Biomacromolecules*, *14*(1), 64–74.

Hein, C. D., Liu, X.-M., & Wang, D. (2008). Click chemistry, a powerful tool for pharmaceutical sciences. *Pharmaceutical Research*, *25*(10), 2216–2230.

Hirota, M., Tamura, N., Saito, T., & Isogai, A. (2010). Water dispersion of cellulose II nanocrystals prepared by TEMPO-mediated oxidation of mercerized cellulose at pH 4.8. *Cellulose*, *17*(2), 279–288.

Huang, J.-L., Li, C.-J., & Gray, D. G. (2014). Functionalization of cellulose nanocrystal films via "thiol–ene" click reaction. *RSC Advances*, *4*(14), 6965.

Kelly, J. A., Shukaliak, A. M., Cheung, C. C. Y., Shopsowitz, K. E., Hamad, W. Y., & MacLachlan, M. J. (2013). Responsive photonic hydrogels based on nanocrystalline cellulose. *Angewandte Chemie International Edition*, *52*(34), 8912–8916.

Khan, M. K., Giese, M., Yu, M., Kelly, J. A., Hamad, W. Y., & MacLachlan, M. J. (2013). Flexible mesoporous photonic resins with tunable chiral nematic structures. *Angewandte Chemie International Edition*, *52*(34), 8921–8924.

Kim, J., Montero, G., Habibi, Y., Hinestroza, J. P., Genzer, J., Argyropoulos, D. S., et al. (2009). Dispersion of cellulose crystallites by nonionic surfactants in a hydrophobic polymer matrix. *Polymer Engineering and Science*, *49*(10), 2054–2061.

Leung, A. C. W., Hrapovic, S., Lam, E., Liu, Y., Male, K. B., Mahmoud, K., et al. (2011). Characteristics and properties of carboxylated cellulose nanocrystals prepared from a novel one-step procedure. *Small*, *7*(3), 302–305.

Malkoch, M., Schleicher, K., Drockenmuller, E., Hawker, C. J., Russell, T. P., Wu, P., et al. (2005). Structurally diverse dendritic libraries: A highly efficient functionalization approach using click chemistry. *Macromolecules*, *38*(9), 3663–3678.

Man, Z., Muhammad, N., Sarwono, A., Bustam, M., Vignesh Kumar, M., & Rafiq, S. (2011). Preparation of cellulose nanocrystals using an ionic liquid. *Journal of Polymers and the Environment*, *19*(3), 726–731.

Mariano, M., El Kissi, N., & Dufresne, A. (2014). Cellulose nanocrystals and related nanocomposites: Review of some properties and challenges. *Journal of Polymer Science B: Polymer Physics*, *52*(12), 791–806.

Morandi, G., Heath, L., & Thielemans, W. (2009). Cellulose nanocrystals grafted with polystyrene chains through surface-initiated atom transfer radical polymerization (SI-ATRP). *Langmuir*, *25*(14), 8280–8286.

Nielsen, L. J., Eyley, S., Thielemans, W., & Aylott, J. W. (2010). Dual fluorescent labelling of cellulose nanocrystals for pH sensing. *Chemical Communications*, *46*(47), 8929–8931.

Nuopponen, M., Meriluoto, A., & Kontturi, E. (2012). *Preparing micro- and nanocrystalline cellulose in the presence of an acid*. Finland: UPM-Kymmene Corporation.

Qin, Z.-Y., Tong, G., Chin, Y. C. F., & Zhou, J.-C. (2011). Preparation of ultrasonic-assisted high carboxylate content cellulose nanocrystals by TEMPO oxidation. *BioResources*, *6*(2), 1136–1146.

Rånby, B. G. (1951). Fibrous macromolecular systems. Cellulose and muscle. The colloidal properties of cellulose micelles. *Discussions of the Faraday Society*, *11*(0), 158–164.

Rieke, P. C., Baer, D. R., Fryxell, G. E., Engelhard, M. H., & Porter, M. S. (1993). Beam damage of self-assembled monolayers. *Journal of Vacuum Science and Technology A*, *11*(4), 2292–2297.

Sadeghifar, H., Filpponen, I., Clarke, S. P., Brougham, D. F., & Argyropoulos, D. S. (2011). Production of cellulose nanocrystals using hydrobromic acid and click reactions on their surface. *Journal of Materials Science*, *46*(22), 7344–7355.

Salajková, M., Berglund, L. A., & Zhou, Q. (2012). Hydrophobic cellulose nanocrystals modified with quaternary ammonium salts. *Journal of Materials Chemistry*, *22*(37), 19798–19805.

Sassi, J.-F., & Chanzy, H. (1995). Ultrastructural aspects of the acetylation of cellulose. *Cellulose*, *2*(2), 111–127.

Shopsowitz, K. E., Hamad, W. Y., & MacLachlan, M. J. (2011). Chiral nematic mesoporous carbon derived from nanocrystalline cellulose. *Angewandte Chemie International Edition*, *50*(46), 10991–10995.

Siqueira, G., Tapin-Lingua, S., Bras, J., da Silva Perez, D., & Dufresne, A. (2010). Morphological investigation of nanoparticles obtained from combined mechanical shearing, and enzymatic and acid hydrolysis of sisal fibers. *Cellulose*, *17*(6), 1147–1158.

Tingaut, P., Hauert, R., & Zimmermann, T. (2011). Highly efficient and straightforward functionalization of cellulose films with thiol-ene click chemistry. *Journal of Materials Chemistry*, *21*(40), 16066.

Van den Berg, O., Schroeter, M., Capadona, J. R., & Weder, C. (2007). Nanocomposites based on cellulose whiskers and (semi)conducting conjugated polymers. *Journal of Materials Chemistry*, *17*(26), 2746–2753.

Yi, J., Xu, Q., Zhang, X., & Zhang, H. (2009). Temperature-induced chiral nematic phase changes of suspensions of poly(*N*,*N*-dimethylaminoethyl methacrylate)-grafted cellulose nanocrystals. *Cellulose*, *16*(6), 989–997.

Zoppe, J. O., Habibi, Y., Rojas, O. J., Venditti, R. A., Johansson, L.-S., Efimenko, K., et al. (2010). *Poly(N-isopropylacrylamide) brushes grafted from cellulose nanocrystals via surface-initiated single-electron transfer living radical polymerization*,